The Stiffness of Skeletal Muscle in Isometric Contraction and Rigor: The Fraction of Myosin Heads Bound to Actin

Marco Linari,* Ian Dobbie,# Massimo Reconditi,* Natalia Koubassova,* Malcolm Irving,# Gabriella Piazzesi,* and Vincenzo Lombardi*

*Department of Physiological Sciences, University of Florence, 50134 Florence, Italy, and #The Randall Institute, King's College London, London WC2B 5RL, England

ABSTRACT Step changes in length (between −3 and +5 nm per half-sarcomere) were imposed on isolated muscle fibers at the plateau of an isometric tetanus (tension T_0) and on the same fibers in rigor after permeabilization of the sarcolemma, to determine stiffness of the half-sarcomere in the two conditions. To identify the contribution of actin filaments to the total half-sarcomere compliance (*C*), measurements were made at sarcomere lengths between 2.00 and 2.15 μm, where the number of myosin cross-bridges in the region of overlap between the myosin filament and the actin filament remains constant, and only the length of the nonoverlapped region of the actin filament changes with sarcomere length. At 2.1 μm sarcomere length, *C* was 3.9 nm T_0^{-1} in active isometric contraction and 2.6 nm T_0^{-1} in rigor. The actin filament compliance, estimated from the slope of the relation between *C* and sarcomere length, was 2.3 nm μm^{-1} T_0^{-1}. Recent x-ray diffraction experiments suggest that the myosin filament compliance is 1.3 nm μm^{-1} T_0^{-1}. With these values for filament compliance, the difference in half-sarcomere compliance between isometric contraction and rigor indicates that the fraction of myosin cross-bridges attached to actin in isometric contraction is not larger than 0.43, assuming that cross-bridge elasticity is the same in isometric contraction and rigor.

INTRODUCTION

Force generation in muscle is generally considered to be due to a structural change, the working stroke, in myosin cross-bridges that are attached to the actin filaments. The working stroke was originally thought to stretch a compliant structure in the cross-bridge itself (Huxley and Simmons, 1971). The thin (actin-containing) filament and the thick (myosin-containing) filament were assumed to be rigid. According to this idea, each cross-bridge acts as an independent force generator, with a compliance corresponding to the amount of instantaneous sliding between thin and thick filaments that reduces the isometric tetanic force (T_0) to zero, ~4 nm (Ford et al., 1977). It follows that the stiffness (the reciprocal of compliance) of the half-sarcomere should be linearly related to the fraction of myosin cross-bridges attached to actin (Huxley, 1980).

Support for this view came from estimates of filament compliance based on the dependence of fiber stiffness on sarcomere length (Ford et al., 1981; Bagni et al., 1990). These experiments led to the conclusion that the contribution of the actin filaments to the half-sarcomere compliance at a sarcomere length that allows full overlap between myosin and actin filaments was less than 20%. However, Julian and Morgan (1981) reported a substantially higher value (~30%) in similar experiments.

In the last few years a large body of experimental evidence has been accumulated which indicates that the actin filament compliance represents a considerably larger fraction, ~50%, of the half-sarcomere compliance. This value was deduced from mechanical measurements on isolated actin filaments (Kojima et al., 1994) and skinned muscle fibers in rigor (Higuchi et al., 1995), and from x-ray measurements of changes in filament periodicities (Huxley et al., 1994; Wakabayashi et al., 1994).

If at full overlap about half of the instantaneous filament sliding required to reduce the isometric force to zero were taken up by shortening of the filaments, the cross-bridge compliance determined in intact single fibers (Ford et al., 1981; Bagni et al., 1990) would have been substantially overestimated and the fiber stiffness would not be linearly related to the fraction of cross-bridges attached to actin filaments. Thus the idea that a large fraction of cross-bridges is attached to actin during isometric contraction would no longer be sustained by the experimental observation that the stiffness during active isometric contraction is a large fraction of that in rigor (Goldman and Simmons, 1977). This fraction is directly related to the force per cross-bridge, a crucial parameter in conventional cross-bridge models with one-to-one coupling between the mechanical and ATPase cycles (Huxley and Simmons, 1971; Goldman and Huxley, 1994; Irving, 1995; Linari and Woledge, 1995; Piazzesi and Lombardi, 1995; Huxley and Tideswell, 1996).

In the work presented here, we determined the compliance of the actin filament and of the cross-bridges in single muscle fibers by measuring, both in isometric contraction

Received for publication 6 August 1997 and in final form 27 January 1998.

Address reprint requests to Dr. Vincenzo Lombardi, Dipartimento di Scienze Fisiologiche, Viale G. B. Morgagni 63, 50134 Firenze, Italy. Tel.: +39-55-4237-307; Fax: +39-55-4379-506; E-mail: lombardi@fisio.unifi.it.

Dr. Koubassova's present address is Institute of Mechanics, Moscow State University, Moscow 119899, Russia.

0006-3495/98/05/2459/15 $2.00

and in rigor, how fiber compliance varies with sarcomere length in the range between 2.00 and 2.15 μm, where the isometric tetanic tension (T_0) is almost constant. In this range the fraction of myosin cross-bridges that can attach to the actin filament is constant, and only the length of the nonoverlapped region of the actin filament changes with sarcomere length, so that the relation between half-sarcomere compliance and sarcomere length gives a direct estimate of the compliance of the actin filament. Combined with an estimate of myosin filament compliance derived from x-ray diffraction experiments, the present results indicate that no more than 43 ± 5% of the myosin heads are attached to actin in an isometric contraction.

MATERIALS AND METHODS

Frogs (*Rana esculenta*) were killed by decapitation and pithing. Single intact fibers (~5 mm long) were dissected from the lateral head of the tibialis anterior muscle in Ringer's solution (115 mM NaCl, 2.5 mM KCl, 1.8 mM $CaCl_2$, 3 mM phosphate buffer at pH 7.1). Connections between tendons and the transducer hooks were made by means of T-shaped aluminum clips (Ford et al., 1977) to minimize end compliance and to obtain optimal alignment between the fiber and the transducer levers.

Experimental set-up

The experimental set-up (Fig. 1) was built around a movable aluminum plate with four pedestals, each carrying a drop of solution (60 μl) held between two coverslips 4 mm wide and 8 mm long (Linari et al., 1993). A hole of appropriate dimensions for illuminating the fiber was drilled in the center of each pedestal. The solution bathing the fiber was changed by moving successive drops into position while the fiber remained on the optic axis. During the experiment the temperature of the drops was maintained at 4°C by feedback control, using a thermistor that continuously monitored the temperature of the aluminum plate. The output from the control circuit fed two thermoelectric modules (CP 1.4-7-10L; Melcor) that were attached to the bottom of the plate. The length change of a 0.7–2.0-mm segment selected in the third of the fiber next to the force transducer end (to minimize the transmission delay between the segment length and force signals) was monitored by means of a striation follower (Huxley et al., 1981; Lombardi and Piazzesi, 1990). The output signal from the striation follower, the mean change in half-sarcomere length in the segment (sensitivity 125 mV/nm/half-sarcomere), was obtained by dividing the difference in sarcomere displacement at the two regions bounding the segment by the number of half-sarcomeres within the segment. Force was measured with a capacitance gauge force transducer (Huxley and Lombardi, 1980) with a resonant frequency of 50 kHz and a time constant of decay of unloaded oscillation of 30–60 μs. A loudspeaker motor (Cecchi et al., 1976; Lombardi and Piazzesi, 1990), able to deliver step length changes complete in ~50 μs, was used to produce steps of ~110 μs duration to avoid excitation of longitudinal oscillations in the fiber. Step length changes were imposed in fixed-end mode (using the feedback signal from the motor position sensor). The length-clamp mode (using the feedback signal from the striation follower output) was not used, because occasional artefacts in the sarcomere length signal could cause irreversible damage to the integrity of the sarcomere structure in the fragile rigor fibers. The tension signal and the mean sarcomere length signal from the selected segment can be used to determine sarcomere stiffness irrespective of the mode of operation of the length servo-system. To electrically stimulate the intact fiber, a pair of platinum wire electrodes (diameter 150 μm) parallel to the fiber were glued to the opposite edges of the coverslips delimiting one of the drops.

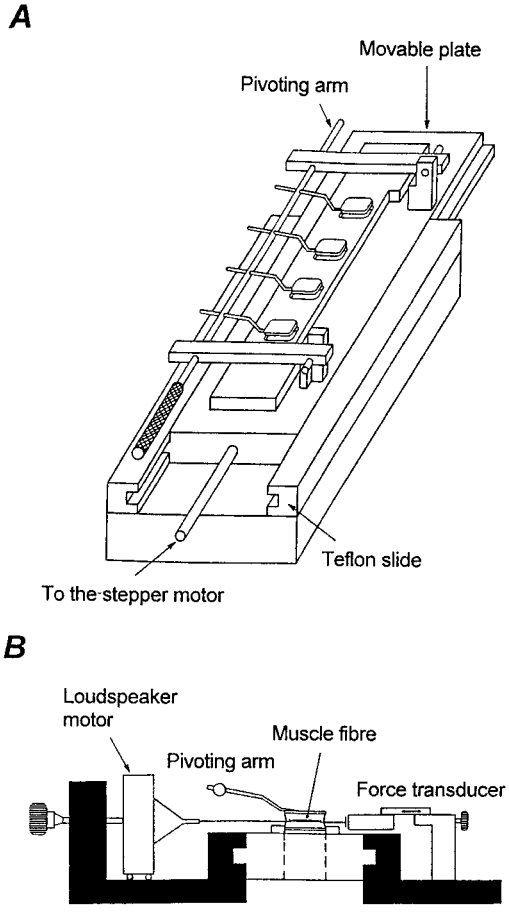

FIGURE 1 Experimental set-up. (*A*) Device for changing solutions. The movable plate was driven by a computer-controlled stepper motor. On the movable plate there were four drops of solution, each held between an upper and a lower coverslip. The upper coverslips were carried on a pivoting arm and were removed to mount and dismount the fiber. In one of the drops two platinum wire electrodes (not shown) were glued parallel to the fiber axis, along the opposite edges of the two coverslips delimiting the drop. This ensured simultaneous contraction of all parts of the fiber length after 0.5-ms pulses of transverse current. (*B*) View along the direction of motion of the movable plate, showing the fiber mounted between the hooks of the loudspeaker motor and the force transducer.

Experimental procedure

An intact fiber was mounted in the experimental trough in Ringer's solution. The sarcomere length (s), width (w), and height at the center of the fiber (h) were measured at 0.5-mm intervals along the fiber with a 40× dry objective (NA 0.60; Zeiss) and an 8× or 25× eyepiece. The cross-sectional area (CSA), determined in 31 fibers at sarcomere length 2.13 ± 0.06 μm (mean ± SD), assuming the fiber cross section was elliptical (CSA = $(\pi/4)wh$), was 5.7 ± 1.9 × 10^{-9} m^2 (mean ± SD). The fiber was stimulated with trains of alternate polarity pulses at a frequency (15–30 Hz) optimal for a fused tetanus. Tetani of 2 s duration were elicited at different sarcomere lengths between 1.98 μm and 2.25 μm. The time interval between successive tetani was 10 min.

After the isometric tetanic plateau tension had been attained, step perturbations in length of −3 to +5 nm per half-sarcomere, measured from the mean changes in the length of the segment monitored by the striation follower, were applied to determine the fiber stiffness. Stiffness was calculated either from the slope of the relation between T_1 (the extreme tension attained during the length step) and the size of the length step (T_1 relation), or from plots of instantaneous force and length changes during

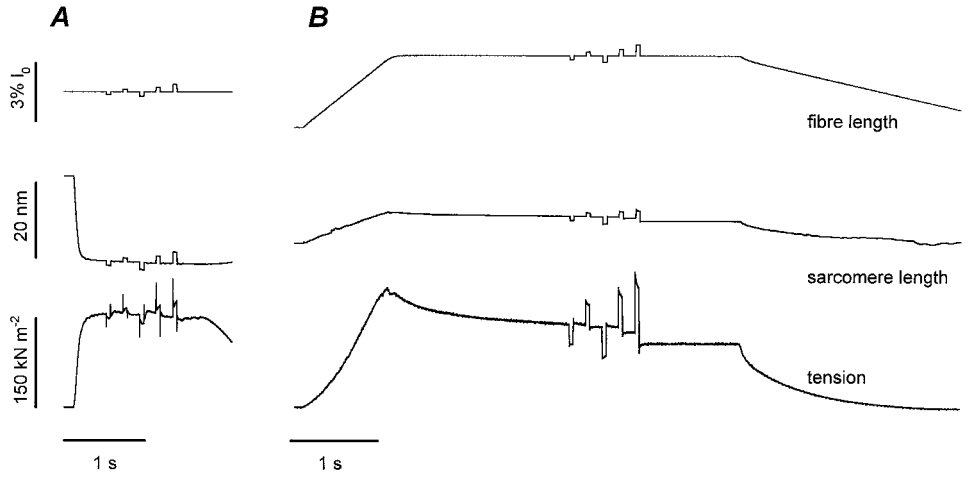

FIGURE 2 Protocol for measuring stiffness at the plateau of an isometric tetanus (*A*) and at a similar tension in rigor (*B*). *Upper traces*: Motor position expressed as a percentage of fiber length (l_0); *middle traces*: sarcomere length change in nm per half-sarcomere; *lower traces*: tension. In rigor the tension just before the first step of the sequence was $0.88T_0$ in this example, where T_0 is the isometric plateau tension in the intact fiber. The same test step sequence was imposed on the fiber at 200-ms intervals in both intact and rigor conditions. The step amplitudes were about -1.0, $+1.0$, -1.5, $+1.5$, and $+2.5$ nm per half-sarcomere. A step of opposite polarity was imposed 50 ms after each test step to return the tension to close to its value before the first step. In this way the tension before each test step differed from that before the first step by less than 4% for the first four test steps and by less than 10% for the fifth test step, both in the intact fiber and in rigor. Tension per unit cross-sectional area (CSA) is expressed relative to CSA in the intact fiber. Isometric tetanus: fiber length, 5.81 mm; length of segment used for sarcomere length measurement by striation follower, 1.33 mm; sarcomere length, 2.03 μm; CSA, 6.0×10^{-9} m^2; temperature, 4.1°C. Rigor: fiber length, 3.86 mm; striation follower segment length, 1.32 mm; sarcomere length, 2.10 μm; CSA, 8.6×10^{-9} m^2; temperature, 4.0°C. The CSA of the permeabilized fiber in relaxing solution was 9.6×10^{-9} m^2.

the step itself. According to previous studies (Ford et al., 1981; Bagni et al., 1990), the stiffness is expected to vary by less than 4% in the range of sarcomere lengths 2.0–2.2 μm. To measure such small changes with sufficient accuracy, it is necessary to minimize the effects of other sources of variation in the measured stiffness, for example, the limited resolution of the striation follower signal and small variations in the isometric tension in a series of tetani. The precision of stiffness measurements at the sarcomere level was enhanced by using a protocol consisting of a train of different sized test steps applied at intervals of 200 ms in each tetanus (Figs. 2 and 3). To minimize differences in tension before the test steps, each test step (marked by a *vertical bar* in Fig. 3) was reversed after 50 ms. Each tetanus at a sarcomere length (s) other than 2.1 μm was preceded and followed by a tetanus at 2.1 μm, and the stiffness at sarcomere length s was calculated relative to the mean of the two neighboring estimates at sarcomere length 2.1 μm. Absolute values for stiffness (K_s) were then obtained by multiplying these relative stiffness values by the average stiffness in all of the measurements at sarcomere length 2.1 μm in that experiment.

After the measurements on the intact fiber had been completed, it was permeabilized in a relaxing solution (Table 1) containing 5 units ml^{-1} of purified α-toxin (Nishiye et al., 1993; kindly provided by Dr K. Török) at 18°C for 20 min. We preferred α-toxin permeabilization to protocols that involved the use of glycerol and detergents, because in preliminary experiments detergents were found to produce weakening of the neuromuscular junction region and increase the probability of the fiber breaking while inducing high tension in rigor. After permeabilization, the fiber was transferred to relaxing solution. Because the α-toxin treatment was found to weaken the tendon attachments, a fiber segment (3–4 mm long) was cut free from the tendons, and new aluminum clips were gently clamped on the segment extremities. The segment ends were glued in air to the clips with shellac dissolved in ethanol (8.3% w/v; Bershitsky and Tsaturyan, 1995) to prevent the fiber segment from slipping out of the clips and to minimize lengthening of the damaged end sarcomeres at the high tension levels induced by stretches in rigor.

Sarcomere length and the dimensions of the fiber segment were measured in relaxing solution after remounting it in the experimental trough at a length just above slack length; both sarcomere length and CSA were found to have increased: in the 31 fibers s was 2.27 ± 0.10 μm (mean ± SD), and CSA was $8.2 \pm 3.0 \times 10^{-9}$ m^2 (mean ± SD). The latter is 44% larger than the value in the intact fiber.

Rigor was induced by MgATP deprivation, using an EDTA rigor solution (Table 1) to chelate Mg^{2+}, because preliminary experiments had shown that α-toxin permeabilized fibers went into rigor very slowly in the

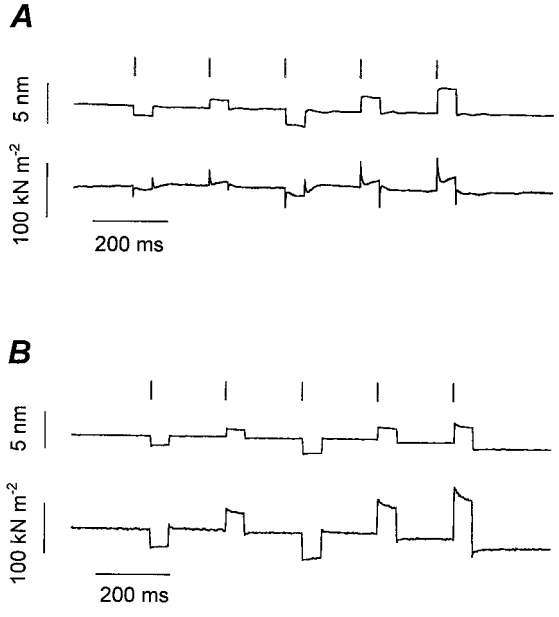

FIGURE 3 Faster time base records of sarcomere length and tension changes in the isometric tetanus (*A*) and rigor (*B*). In each panel the upper trace is sarcomere length in nm per half-sarcomere, and the lower trace is tension. The vertical bars above the sarcomere length signals mark the steps used for stiffness measurements (test steps). From the same records as Fig. 2.

TABLE 1 Solution compositions

Solution name	Na_2ATP (mM)	$MgCl_2$ (mM)	EGTA (mM)	EDTA (mM)	Na_2CP (mM)	CPK (mg/ml)	BDM (mM)	TES (mM)	GLH (mM)
Relaxing	5.4	7.7	25	—	19.1	1.0	20	100	10
Prerigor	0.5	3.0	10	—	—	—	20	100	—
Rigor-BDM	—	—	—	34.0	—	—	20	100	—
Rigor	—	—	—	34.0	—	—	—	100	—

CP, creatine phosphate; CPK, creatine phosphokinase; BDM, 2,3-butanedione monoxime; TES, *N*-tris[hydroxymethyl]methyl-2-aminoethane sulfonic acid; GLH, glutathione; pH of all solutions, 7.1 at 20°C, adjusted with KOH ($2–12 \times 10^{-3}$ M). Ionic strength: relaxing, 200 mM; rigor-BDM and rigor, 150 mM; prerigor, 100 mM. EDTA was obtained from Fluka (Buchs, Switzerland). All other chemicals were obtained from Sigma.

presence of Mg^{2+}. We tested the possibility that our rigor stiffness measurements were affected by the use of the relatively low ionic strength EDTA rigor solution by comparing sarcomere stiffness in EDTA rigor solution (Table 1) with that in a more conventional Mg rigor solution containing 1.7 mM $MgCl_2$; 20 mM EGTA; 37.9 mM 1,6-diaminohexane-*N*,*N*,*N*′,*N*′-tetraacetic acid; 100 mM *N*-tris-(hydroxymethyl)methyl-2-aminoethanesulfonic acid; 10 mM glutathione; ionic strength: 200 mM. For these comparisons we used the longer fibers from the medial head of the tibialis anterior muscle, in which a segment free from neuromuscular junction can be isolated after α-toxin treatment. Rigor stiffness was measured as usual in EDTA rigor and then, after treatment with Triton X-100 (0.5% for 10 min), in Mg rigor. The stiffness measured in a range of forces from 0.2 to 0.8 T_0 did not differ significantly in the two rigor solutions. The ratio of Mg rigor to EDTA rigor stiffness was 1.07 ± 0.09 (mean ± SEM) ($p > 0.4$ with *t*-test for the differences in three experiments).

The procedure to induce rigor was developed from that described by Higuchi et al. (1995), which preserved the regularity of the striation pattern along the fiber and allowed the sarcomere length in rigor to be set at a chosen value. Starting with the fiber segment in relaxing solution, the segment length was set for the desired sarcomere length value in rigor; usually the fiber went slack. The fiber was then transferred to a prerigor solution containing 2,3-butanedione monoxime (BDM) (Table 1) for 10 min at 10°C. The temperature was reduced to 0°C, and the fiber was transferred to rigor-BDM solution (Table 1) for 10 min. In these conditions the fiber took up any slack without developing irregularities in the striation pattern and became stiff without developing detectable force. The half-time of stiffness development (measured by the instantaneous tension change in response to a small stretch) was ~2 min.

The fiber was then transferred to rigor solution without BDM (Table 1) and allowed to warm up to 4°C, and *s* and CSA were measured again. In the 31 fibers *s* was 2.14 ± 0.08 μm and CSA was $7.2 \pm 2.3 \times 10^{-9}$ m^2 (mean ± SD). The CSA value was 27% larger than in the intact fibers.

To avoid the effect of tension on stiffness estimates in rigor (Higuchi et al., 1995), stiffness in rigor was measured at the same steady force as that at the isometric tetanus plateau. To attain a steady force level in rigor comparable to the isometric plateau force in the intact fiber (T_0), the fiber was lengthened by a slow ramp (duration ~1.5 s). A train of length steps (Fig. 2 *B*) was applied to the fiber 2 s after the end of the ramp to determine rigor stiffness. The slow ramp stretch was reversed 1 s after the last step of the train. Sometimes irreversible yielding of part of the segment developed progressively in repeated cycles of ramp lengthening, as indicated by the segment being slack after the ramp was reversed. In these cases, before the next ramp stretch was applied, the fiber was set just taut (tension less than 0.1 T_0) by using the micromanipulator carrying the motor. The experiment was stopped when the striation follower signal was no longer reliable because sarcomere translation could not be measured continuously in one of the regions bounding the selected segment. Because of the fragility of the rigor fibers, data were usually collected for only four to six cycles in rigor. In a few fibers it was possible to obtain rigor stiffness measurement at two different sarcomere lengths in the same preparation; in these fibers, after increasing the temperature to 10°C, the fiber segment was transferred to relaxing solution and the segment length was adjusted for the new sarcomere length. A second cycle of rigor induction in the fiber segment was then initiated.

For the analysis reported below, we used only 10 fibers of the 31 fibers tested, all with rigor solution according to Table 1. In these fibers, throughout all phases of the experiment (including rigor), the striation pattern remained ordered and the sarcomere length along the segment under inspection did not vary by more than ±5%. Stiffness measurements in the whole range of sarcomere lengths, required to determine the relation between compliance and sarcomere length in the intact fiber, were collected in only 5 of the 10 fibers.

Data recording

Tension and motor position were monitored continuously on a chart recorder (speed 10–25 mm/s). Tension, motor position, and sarcomere length signals were recorded at sampling intervals of 5–10 μs with a digital oscilloscope (Nicolet ProSystem 20) and at sampling intervals of 1 ms with an A/D card (Computerscope EGAA; RC Electronics) in a 386/33 PC. Traces from the digital oscilloscope were stored on diskettes for subsequent analysis. The responses were measured directly on the Nicolet oscilloscope by means of its internal cursors, and on the PC with the EGAA software.

RESULTS

Tension transients in isometric contraction and in rigor

Tension transients in response to length steps of −3 to +5 nm per half-sarcomere, measured from the mean change in sarcomere length in the fiber segment monitored by the striation follower, were elicited both in the intact fiber at the plateau of an isometric tetanus (tension T_0; Fig. 2 *A*) and in the same fiber in rigor at a tension close to T_0 (Fig. 2 *B*). The high force value in rigor was obtained by applying a slow ramp stretch of 2–6% of the fiber length, which corresponded to only 5–10 nm per half-sarcomere in the selected segment because of the large compliance and "give" of the attachments. In the ~2-s period between the end of the ramp and the start of the train of length steps, the mean sarcomere length in the segment shortened by 0.5–2 nm. This shortening progressively slowed and was accompanied by a tension drop of 10−40% of T_0 with the same time course. The slow stress relaxation of segment length and force after the ramp stretch are probably the consequence of further slow give in the attachments.

In active isometric contraction, the step length change elicits a tension transient (Huxley and Simmons, 1971) composed of an instantaneous "elastic" response (phase 1) followed by a complex recovery toward the original tension

value (Figs. 3 *A* and 4 *A*). Because the test step was followed, after 50 ms, by a step in the opposite direction, only the faster components of the tension recovery are observed in the present experiments. The tension transients after step releases (first and third test steps; Fig. 3 *A*) are faster than those after stretches, and the quick recovery (phase 2), the transient reversal of recovery (phase 3), and the beginning of the slow recovery (phase 4) are observed. For step stretches (second, fourth, and fifth test steps; Fig. 3 *A*) the tension transient becomes progressively slower with increasing step size, and only phases 2 and 3 are observed. In rigor (Figs. 3 *B* and 4 *B*) there is much less tension recovery after the elastic response.

The sarcomere length changes after the larger length steps were clearly different in tetanic contraction (Figs. 3 *A* and 4 *A*) and in rigor (Figs. 3 *B* and 4 *B*). In the tetanus, the quick tension recovery was accompanied by a further change in segment length in the same direction as that during the step, as expected in fixed-end conditions because of extension or shortening of the tendon attachments during tension recovery by cross-bridges after a release or a stretch, respectively. In rigor the change in segment length after the length step was generally in the direction opposite that during the length step, indicating "give" of some part of the fiber outside the segment where sarcomere length was recorded. This effect was larger after step stretches and is responsible for most of the tension recovery after the step, which has a time course similar to that of the segment length change (Fig. 3 *B*). This recovery process is similar to the slow stress relaxation after a ramp stretch in rigor (Fig. 2 *B*).

The fast component of tension recovery, corresponding to phase 2 of the tension transient, is much smaller in rigor than in the isometric tetanus. A more quantitative comparison of the fast tension recovery in the isometric tetanus and in rigor would require measurements of tension transients under segment length control, and is beyond the scope of the present study.

The main aim of the present work is to make precise measurements of instantaneous stiffness (phase 1 of the tension transient) in isometric contraction and in rigor. This can be done by recording tension and changes in the mean sarcomere length in the segment under inspection in response to applied length steps in fixed-end conditions.

Stiffness measurements at 2.1-μm sarcomere length

When the same step change in sarcomere length is imposed in isometric contraction and rigor, the instantaneous tension response is larger in rigor (Fig. 4), indicating the higher stiffness of the rigor fiber. The elastic characteristics of the half-sarcomere can be represented by a plot of the extreme tension attained during a length step (T_1) against the size of the length step (the T_1 relation; Huxley and Simmons, 1971).

Fig. 5 shows T_1 relations for the same fiber in an isometric tetanus (*open circles*) and in rigor (*triangles*) at the same sarcomere length (2.1 μm). The T_1 points, normalized as described below for the variation in the tension before each length step, are expressed relative to T_0, the steady tension in isometric contraction before the first step. The effects of the small variation in tension before each test step were eliminated by multiplying each T_1 point by the factor $\bar{T}_i/T_i$, where T_i is the tension just before each step (the first T_i value corresponds to T_0) and $\bar{T}_i$ (the *point on the ordinate* in Fig. 5) is the mean of the five T_i values in each train.

In the present experiments the length changes were complete in 110 μs, and all of the releases were smaller than 3 nm/half-sarcomere. Thus the effect of fast tension recovery

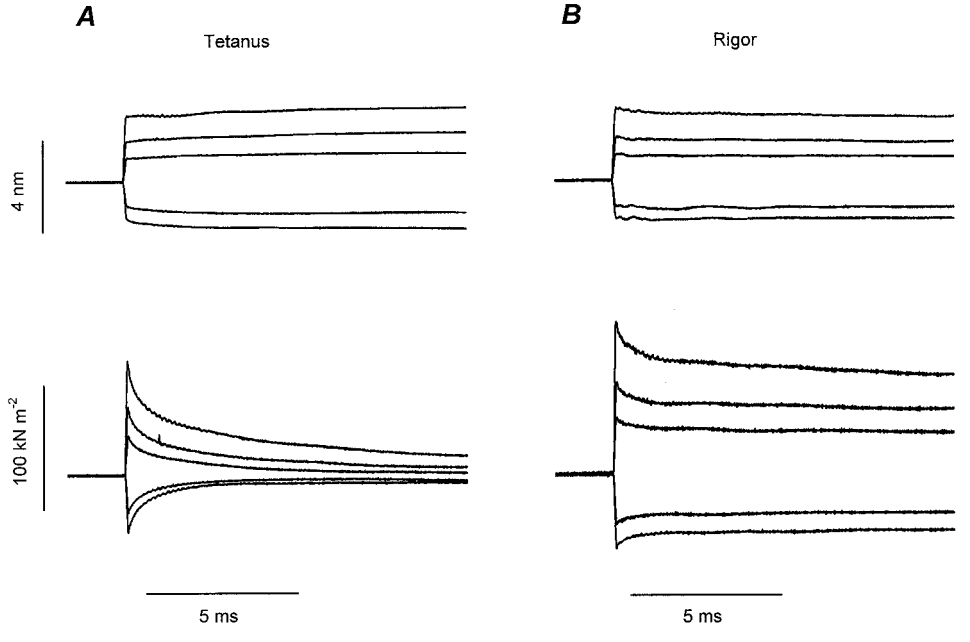

FIGURE 4 Superimposed sarcomere length and tension signals from different size length steps. (*A*) Isometric tetanus; (*B*) rigor. *Upper row*: Sarcomere length changes; *lower row*: tension changes. From the same fiber as Fig. 2.

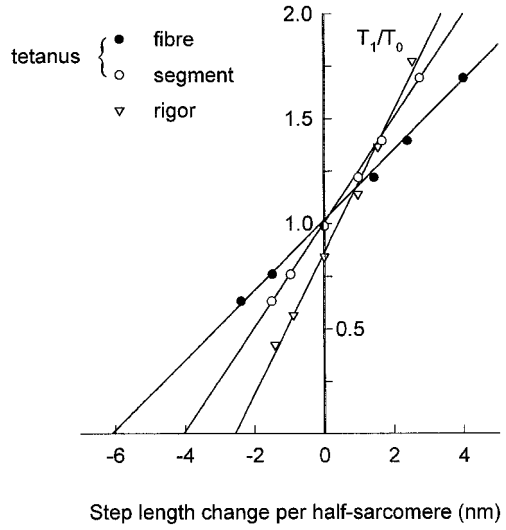

FIGURE 5 T_1 relations in isometric contraction and in rigor. The extreme tension attained during the length step (T_1, normalized by T_0 as explained in the text) at the plateau of an isometric tetanus (○, ●) and in rigor (▽) at 2.1 μm sarcomere length, plotted against the length change measured at the same time as T_1. ○, ▽, Length signal from the striation follower; ●, length signal from the motor position sensor. The continuous lines are linear regression lines fitted to each set of points. The slopes for the segment length data (○, ▽), which give the half-sarcomere stiffness in units of T_0 nm^{-1}, were 0.249 ± 0.005 (mean ± SEM) in isometric contraction and 0.337 ± 0.013 in rigor. The fiber stiffness in isometric contraction (which includes the contribution of the tendon) was 0.167 ± 0.004 T_0 nm^{-1}, 33% less than the segment stiffness. Same fiber as in Fig. 2. Sarcomere length: intact fiber, 2.10 μm; rigor fiber, 2.10 μm. The rigor tension was 0.85 ± 0.02 T_0 (mean ± SEM, $n = 5$).

during the length step on the T_1 values (Ford et al., 1977) was negligible, and the T_1 relation was considered to be linear (Fig. 5). The slope of the T_1 relation, determined by linear regression, was used to measure the instantaneous stiffness (K) of the segment under inspection. In five fibers at 2.1 μm sarcomere length, K in isometric contraction was 62 ± 5% (mean ± SEM) of that in rigor (Table 2).

The intercept of the T_1 relation on the length axis (Y_0 in Ford et al., 1977) represents the extent of instantaneous shortening necessary to reduce the force from T_0 to zero and measures the compliance of the half-sarcomere (C). The mean value of C was 4.17 ± 0.05 nm/half-sarcomere/T_0 (SEM, $n = 5$) in isometric contraction, and 2.56 ± 0.16 nm/half-sarcomere/T_0 ($n = 4$) in rigor.

The T_1 relation in the isometric tetanus for the whole fiber is shown by the filled circles in Fig. 5. For comparison with the T_1 relation obtained from changes in segment length, the fiber length change was expressed in units of nm/half-sarcomere by multiplying its value as a fraction of fiber length by the average half-sarcomere length in the fiber. The T_1 relation was less steep than that for the segment (*open circles*) because of the contribution of tendon compliance. C for the whole fiber was 6.21 ± 0.31 nm/half-sarcomere/T_0. In the five fibers the fiber stiffness was 33 ± 2% lower than the segment stiffness (Table 2).

Instantaneous tension-length relations

The fiber stiffness in isometric contraction, as measured with length steps of 100–200 μs duration, is dominated by the elastic behavior of the sarcomeres and is not significantly affected by viscosity (Ford et al., 1977; Piazzesi et al., 1992). To establish whether the rigor stiffness also arises from a purely elastic response, the tension at 5- or 10-μs intervals during the length steps was plotted against the segment length change at the same instant, in both isometric contraction (Fig. 6 *A*) and rigor (Fig. 6 *B*). The duration of the length step was fixed, so the larger steps correspond to larger velocities, and the presence of a significant viscosity would displace the instantaneous tension values downward for larger releases and upward for larger stretches (Ford et al., 1977). In both active and rigor conditions, the points belonging to different step sizes were found to superimpose, indicating the absence of a significant viscous component at the sampling rate used here. Thus the active and rigor stiffnesses show an almost pure elasticity, and their values can be directly compared.

The intercept of the instantaneous tension-length relation on the length axis was obtained by extrapolating the line obtained by linear regression of the first 10 points (corresponding to the first 100 μs) during the length step for all five length step amplitudes (Fig. 6). In six fibers at ~2.1 μm sarcomere length, the values of C, calculated from the intercept on the length axis, were 6.6 ± 1.1% and 0.9 ± 1.9% (mean ± SEM) less that those derived from the T_1 relation in isometric contraction and rigor, respectively. The instantaneous tension-length relation is expected to yield a smaller value of C than the T_1 relation in isometric contraction because of truncation of T_1 by quick tension recovery during the length step (Ford et al., 1977). This truncation is effectively absent in rigor, because the fastest components of the quick recovery are suppressed. The stiffness of the half-sarcomere derived from instantaneous tension-length plots at 2.1-μm sarcomere length in isometric contraction was 66 ± 5% of that in rigor (mean ± SEM, $n = 6$).

TABLE 2 Comparison of stiffness in isometric contraction and in rigor at ~2.1 μm sarcomere length

	Sarcomere length (μm)	$\bar{T}_i/T_0$	Segment stiffness (T_0 nm^{-1})	Fiber stiffness (T_0 nm^{-1})
Intact ($n = 5$)	2.128 ± 0.002	0.999 ± 0.010	0.240 ± 0.003	0.161 ± 0.008
Rigor ($n = 4$)	2.120 ± 0.009	0.945 ± 0.043	0.390 ± 0.024	

Data are obtained from T_1 relations and expressed as mean ± SEM. $\bar{T}_i/T_0$ is the average tension before the test step as explained in the text.

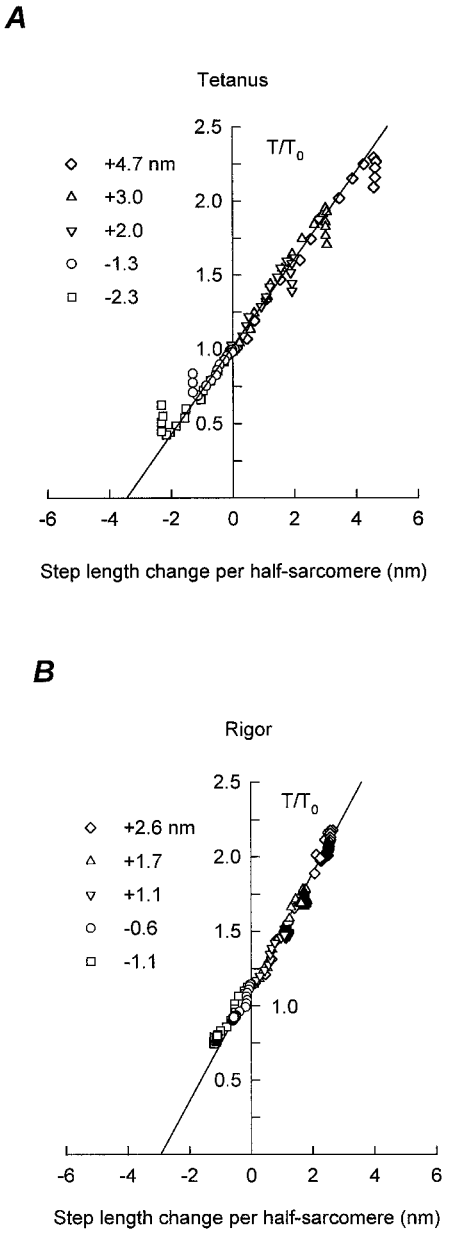

FIGURE 6 Instantaneous tension-length relation during steps of different sizes imposed in isometric contraction (*A*) and in rigor (*B*). The rigor tension before the first step was $1.1T_0$. Tension values for each step were normalized as T/T_0 as described in the text. The amplitudes of the length steps in nm per half-sarcomere shown in the symbol key were measured at the time of the extreme tension change (T_1). The time interval between points was 10 μs. The intercept on the abscissa was 3.46 nm in *A* and 2.92 nm in *B*. The corresponding values of *C*, the half-sarcomere compliance normalized for T_0, were 3.46 nm T_0^{-1} and 2.65 nm T_0^{-1}. Intact fiber: length of segment used for striation follower, 1.27 mm; sarcomere length, 2.04 μm; CSA, 6.2×10^{-9} m^2. Rigor: length of segment used for striation follower, 1.28 mm; sarcomere length, 2.06 μm; CSA, 9.8×10^{-9} m^2. Temperature, 4.1°C.

Dependence of sarcomere compliance on sarcomere length in the isometric tetanus

In the plateau region of the isometric tension–sarcomere length relation (in the sarcomere length range from ~2.0 to 2.2 μm), the number of myosin cross-bridges overlapped by actin filaments is constant. If the actin filaments are compliant, the stiffness of the half-sarcomere (K) is expected to vary with sarcomere length in this range solely as a result of the change in the length of the nonoverlapped actin filaments in the I-band (Ford et al., 1981; Bagni et al., 1990; Higuchi et al., 1995), assuming that stiffness is not significantly affected by the small change in interfilamentary spacing. In this sarcomere length range, the compliance of the half-sarcomere C ($= 1/K$) is expected to be linearly related to sarcomere length (equation A10 of Ford et al., 1981), so it is convenient to present the experimental results in terms of compliance rather than stiffness.

Analysis of compliance data was limited to the sarcomere length range 2.00–2.17 μm, where isometric tetanic tension was within 2% of its maximum value at 2.10 μm (Fig. 7 *A*). In the tension-sarcomere length relation originally reported by Gordon et al. (1966) for semitendinosus muscle fibers, the plateau region was from 2.05 to 2.25 μm. However, in tibialis anterior fibers, as used here, the plateau of the tension-length relation is shifted to the left by ~0.1 μm and is restricted to a smaller range of sarcomere lengths (Bagni et al., 1988, 1990), probably as a result of variation in actin filament lengths (Bagni et al., 1990). In our experiments there was no detectable difference in isometric tetanic tension between 2.05 and 2.10 μm, and for purposes of the compliance analysis we considered the points at 2.00 and 2.15 μm, where tension is within ±1% of the mean value, to be included in the plateau region.

In this plateau region, the contributions of myosin filament and cross-bridge compliance can be considered to be constant, and the relation between half-sarcomere compliance (C) and sarcomere length (s) can be written as

$$C = \frac{c_A}{2}(s - s_0) + C_0 \quad (1)$$

where c_A is actin filament compliance per unit length, s_0 is the reference sarcomere length (2.1 μm), and C_0 is the half-sarcomere compliance at $s = 2.1$ μm. C_0 depends on the compliances of actin and myosin filaments, cross-bridges, and the Z-line (see Appendix, Eq. A4).

Half-sarcomere compliance in isometric contraction was found to increase with increasing sarcomere length in the range 2.00–2.17 μm (Fig. 7 *B*). A similar increase was observed for compliance values obtained using the segment length signal from the striation follower (*open symbols*) and those obtained using the motor position signal (*filled symbols*) to monitor changes in fiber length. The length changes for the whole fiber have been expressed in nm/half-sarcomere, as described previously for the T_1 relation. The fiber compliance was larger than the segment compliance, as a result of the contribution of tendon compliance.

The slope of the relation between half-sarcomere compliance and sarcomere length ($c_A/2$, Eq. 1) was determined by linear regression of the data for each fiber (Fig. 7 *B*, *continuous lines*). The resulting values of c_A in isometric

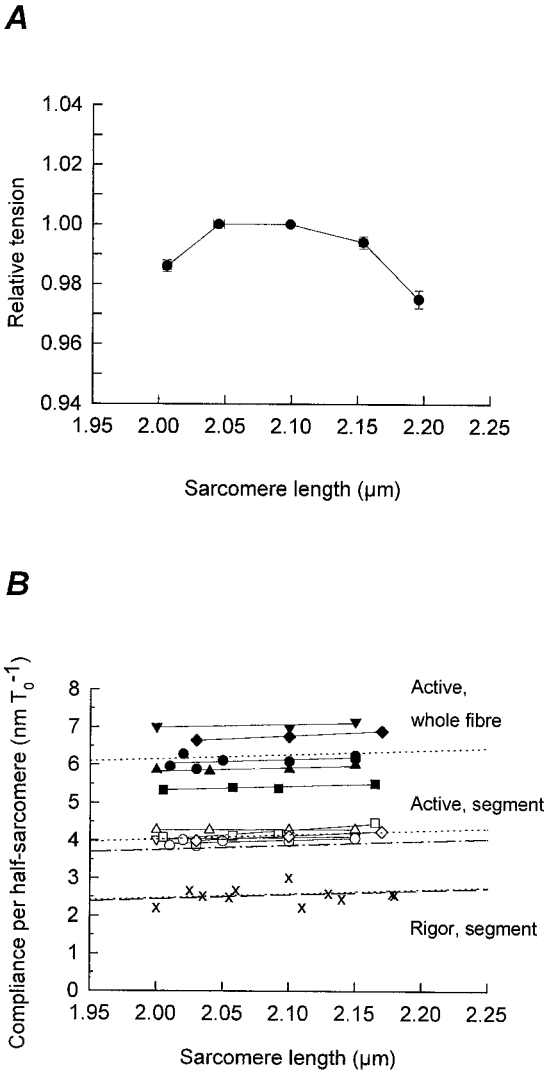

FIGURE 7 Dependence of isometric tetanic tension (*A*) and half-sarcomere compliance (*B*) on sarcomere length. (*A*) Isometric tetanic tension, relative to that at 2.1 μm, obtained by grouping measurements at different sarcomere lengths into classes 0.05 μm wide. Data are mean ± SEM from five fibers. In some cases the error bar is smaller than the symbol. (*B*) Half-sarcomere compliance, *C*, in isometric contraction and in rigor, calculated from the intercept of T_1 relations on the length axis, plotted against sarcomere length. *Open symbols*: Values of *C* in isometric contraction from the segment length change ("active, segment"); *filled symbols*: values from the movement of the motor hook ("active, whole fiber"). Corresponding symbols in the segment and fiber data were obtained from the same preparation, and these are the same five fibers used in *A*. The continuous lines were obtained by linear regression on the data from each fiber. *Crosses*: Values of *C* in rigor using the segment length change ("rigor, segment") obtained from these five plus five other fibers. The dotted line superimposed on the "active, whole fiber" data was calculated using Eq. 1 in the text and the mean values of c_A (2.32 nm $\mu m^{-1}\ T_0^{-1}$) and C_0 (6.27 nm T_0^{-1}). The dotted lines superimposed on the "active, segment" and "rigor, segment" data were obtained by fitting Eq. 1 to pooled data for each of these conditions, assuming the value of c_A estimated from the whole fiber data (2.32 nm $\mu m^{-1}\ T_0^{-1}$). C_0 was 4.15 nm T_0^{-1} for the "active, segment" data and 2.58 nm T_0^{-1} for the "rigor, segment" data. The dot-dashed line ("active, segment") and the dashed line ("rigor, segment") were obtained by shifting down the *C* values from the dotted lines by 0.28 nm (active) and 0.02 nm (rigor), respectively, to take into account the effect of truncation of the T_1 by early tension recovery, as explained in the text.

contraction were 2.47 ± 0.85 nm $\mu m^{-1}\ T_0^{-1}$ (mean ± SEM, $n = 5$) for the segment length data, and 2.32 ± 0.34 nm $\mu m^{-1}\ T_0^{-1}$ for the fiber length data. These values are not significantly different ($p > 0.5$, *t*-test).

The much larger vertical spread of the compliance data obtained from fiber length changes is due to variation in tendon compliance between preparations. The smaller vertical spread of the compliance data obtained from segment length changes was not correlated to that obtained from fiber length changes, and is probably due to errors in the striation follower signal related to sarcomere length inhomogeneity. These errors are probably responsible for the larger SEM of the estimate of c_A from the segment length data, which is more than twice that for the fiber length data. Therefore we consider the estimate of c_A from the fiber length data, 2.32 nm $\mu m^{-1}\ T_0^{-1}$, to be the more reliable. This value was used to calculate the dotted lines superposed on the two sets of data for active contraction in Fig. 7 *B*.

Half-sarcomere compliance at sarcomere length 2.1 μm (C_0) was 6.27 ± 0.29 nm T_0^{-1} for the fiber length data (mean ± SEM, obtained from the individual regressions through each set of *filled symbols*). For the segment length data C_0 was estimated to be 4.15 ± 0.03 nm T_0^{-1} by fitting Eq. 1 to the pooled data with $c_A = 2.32 \pm 0.34$ nm $\mu m^{-1}\ T_0^{-1}$. The difference between C_0 values obtained from the fiber length and segment length data, corresponding to the vertical displacement between the two dotted lines in Fig. 7 *B*, was 2.12 nm T_0^{-1}, and this is due to the contribution of tendon compliance. The value of C_0 for the segment length data, 4.15 nm T_0^{-1}, is very close to that determined in a previous section; the segment stiffness obtained from T_1 relations was 0.240 T_0 nm^{-1} (Table 2), corresponding to $C_0 = 4.17$ nm T_0^{-1}. These values also agree with previous results obtained under the same conditions (Lombardi and Piazzesi, 1990; Piazzesi et al., 1992). We showed in the previous section that the compliance obtained from the T_1 relation in an isometric tetanus is overestimated by 6.6 ± 1.1% compared with that obtained from instantaneous tension-length plots. Thus the corrected value of C_0 should be 3.88 ± 0.05 nm T_0^{-1}, and the *C*:*s* relation should be shifted downward accordingly (shown as the *dot-dashed line under the segment length data* in Fig. 7 *B*).

Dependence of sarcomere compliance on sarcomere length in rigor

The dependence of the half-sarcomere compliance, *C*, on sarcomere length in rigor is shown in Fig. 7 *B* (*crosses*) for the five fibers studied in active isometric contraction plus other five fibers. As discussed in Materials and Methods, it is difficult to measure *C* in rigor at two different sarcomere lengths in the same fiber, and this was possible in only one of the fibers in Fig. 7 *B*. Therefore we used the pooled data from the 10 fibers in rigor for regression analysis of the compliance-sarcomere length relation (Eq. 1). The resulting value of c_A was 1.2 ± 2.3 nm $\mu m^{-1}\ T_0^{-1}$, and C_0 was

2.58 ± 0.07 nm T_0^{-1}. Although the value of c_A is not significantly different from that measured in isometric contraction, the large standard error means that the rigor data cannot be used to estimate c_A. The dotted line through the rigor data in Fig. 7 *B* is a least-squares fit obtained with c_A set to 2.32 nm μm^{-1} T_0^{-1}, the value in isometric contraction. The value of C_0 obtained from this fitting procedure was 2.58 ± 0.07 nm T_0^{-1}, the same value as C_0 obtained by linear regression with c_A as a free parameter. This value is also close to that determined from the T_1 relation at sarcomere length 2.1 μm (segment stiffness 0.390 T_0 nm^{-1} (Table 2), corresponding to C_0 = 2.56 nm T_0^{-1}).

There is very little truncation of T_1 by quick tension recovery in rigor, and the compliance determined from the T_1 relation is overestimated by only 0.9 ± 1.9%, as discussed above. The dashed line through the rigor data in Fig. 7 *B* was obtained by reducing C_0 in Eq. 1 by 0.9% (from 2.58 ± 0.07 to 2.56 ± 0.08 nm T_0^{-1}). The vertical displacement between the compliance:sarcomere length relations for isometric contraction (*dot-dashed line*) and rigor (*dashed line*) was 1.31 nm T_0^{-1}. This displacement is likely to be due to the reduced contribution of myosin cross-bridge compliance in rigor as a consequence of the larger number of cross-bridges attached to actin.

DISCUSSION

Sarcomere stiffness in isometric contraction and in rigor

The stiffness of the half-sarcomere in single muscle fibers at 2.1 μm sarcomere length, determined from step perturbations in sarcomere length, was 0.240 T_0 nm^{-1} in an isometric tetanus and 0.390 T_0 nm^{-1} in rigor (Table 2). The corresponding values from linear regression of half-sarcomere compliance against sarcomere length were (1/4.15 =) 0.241 T_0 nm^{-1} and (1/2.58 =) 0.388 T_0 nm^{-1}, respectively. Thus the half-sarcomere stiffness in an isometric tetanus was 62 ± 5% of that in rigor. This parameter becomes 66 ± 5%, using the slope of the instantaneous tension-sarcomere length relations (1/3.88 = 0.258 T_0 nm^{-1} in the isometric tetanus and 1/2.56 = 0.391 T_0 nm^{-1} in rigor).

These estimates of the active:rigor stiffness ratio are similar to that reported by Yamamoto and Herzig (1978) but ~15% smaller than that reported by Goldman and Simmons (1977). The difference may be related to the application of length steps from a low steady rigor tension in Goldman and Simmons' experiments, because rigor stiffness increases with static tension (Higuchi et al., 1995, and our unpublished results). This effect was avoided in the experiments of Yamamoto and Herzig and in the present experiments by measuring rigor stiffness at a tension close to T_0.

Another distinct feature of the present experiments is that the rigor stiffness was compared with the stiffness of the active intact fiber, whereas Goldman and Simmons (1977) measured active stiffness in skinned fibers. Skinning causes lateral expansion of the filament lattice. The T_1 relation in active skinned fibers from frog muscle is nonlinear, and osmotic compression of the filament lattice makes the T_1 relation more linear and increases the stiffness (Goldman and Simmons, 1986). These problems were avoided in the present experiments by measuring active stiffness in the intact fibers. The stiffness of active intact fibers is independent of the tonicity of the bathing solution in the range 0.8–1.44 times that of normal Ringer's solution (Månsson, 1993; Piazzesi et al., 1994), which alters the filament lattice spacing by 16% (Bagni et al., 1994).

The cross-sectional area of the fibers was ~27% larger in rigor than in the intact fibers, suggesting that the interfilamentary distance was ~13% larger in rigor. X-ray diffraction measurements using the same protocol as the present experiments showed that the filament lattice spacing was 16 ± 5% (mean ± SD, n = 3) larger in rigor than in the intact resting fiber (our unpublished results). Given the insensitivity of the stiffness of the active intact fiber to lattice spacing changes of this magnitude, it seems unlikely that this difference has a substantial effect on the stiffness measured here.

Assuming that all myosin cross-bridges are attached to actin and are under tension in rigor (Cooke and Franks, 1980; Thomas and Cooke, 1980; Lovell et al., 1981), the active:rigor stiffness ratio can be used to estimate the fraction of attached cross-bridges in active contraction, subject to the following conditions:

1. Each attached cross-bridge exhibits the same type of instantaneous elasticity in isometric contraction and in rigor.

2. The compliance of the other structures in the half-sarcomere (e.g., the myosin and actin filaments) can be determined.

Elasticity of cross-bridges in isometric contraction and in rigor

The viscoelastic behavior of cross-bridges in isometric contraction and in rigor was examined by comparing the instantaneous tension-length relations (Fig. 6). In both cases the plots from length steps of different amplitudes superimposed, indicating that in both the active and rigor conditions the elastic response at 5–10 μs time resolution is not significantly influenced by viscosity.

It is possible that the stiffness of an individual myosin cross-bridge attached to actin is not a constant, but varies as the cross-bridge progresses through the force-generating cycle toward the rigor state. Recent time-resolved x-ray diffraction experiments (Lombardi et al., 1995) suggest that cross-bridge compliance is located at least partly within the myosin head itself, in the bending of the light chain region of the head or in angular distortion of the actin-myosin bond. One mechanism by which this might lead to a state-dependent compliance would be if the cross-bridge in rigor were oriented less perpendicular to the filament axis (Reedy

et al., 1965; Piazzesi et al., 1997a), increasing its bending stiffness in response to an axial strain.

On the other hand, not all of the cross-bridges may contribute fully to the rigor stiffness. According to a recent model that considers the role of the two heads in each myosin molecule (Huxley and Tideswell, 1997), it is possible that the second head cannot bind strongly when the first is attached. More generally, although it is well established that all myosin heads are attached to actin in rigor, it is possible that some of these are not bearing tension and do not respond to an applied length step.

The resolution of these uncertainties requires further experiments. In the rest of this paper we will retain the simplest assumption that the elasticity of a single cross-bridge is the same in the isometric contraction and in rigor.

Filament compliance

Compliance, the reciprocal of stiffness, is a convenient parameter for describing the elasticity of structural components of the sarcomere that are mechanically in series with the cross-bridges. In fact, cross-bridges and myofilaments are interconnected in a complex series-parallel arrangement. The elements that are mechanically in series are the Z-line, the zone of nonoverlapped actin filaments, the zone of filament overlap in which cross-bridges link actin and myosin filaments, and the bare zone of the myosin filaments. The compliances of these elements add to give the total half-sarcomere compliance. In the absence of evidence for compliance in the Z-line in the following discussion, we assume that the compliance of the Z-line is zero. We first consider the compliance of the actin and myosin filaments, then deduce the compliance of the cross-bridges.

Compliance of the actin filaments

The compliance of the actin filaments was estimated from the relationship between half-sarcomere compliance and sarcomere length in the sarcomere length range 2.00–2.15 μm, where the isometric tetanic tension varied by less than $\pm$1% and the number of attached cross-bridges can be considered to be constant. In this region the compliance of the overlap zone is constant, and the variation in the half-sarcomere compliance with sarcomere length is due to the different length of the zone of nonoverlapped actin filaments. In the active fiber the compliance of the actin filament per unit length, c_A, was estimated to be 2.32 $\pm$ 0.34 nm $\mu m^{-1}\ T_0^{-1}$ from the slope of the relation between fiber compliance and sarcomere length. This estimate is not affected by the contribution of the tendons to fiber compliance, because tendon compliance is independent of sarcomere length.

The strain in the actin filament depends on its compliance and on the distribution of the force along it, increasing from zero opposite the bare zone to a maximum in the I-band (Fig. 8 *B*). The average strain in the actin filament ($\bar{S}_A$) at

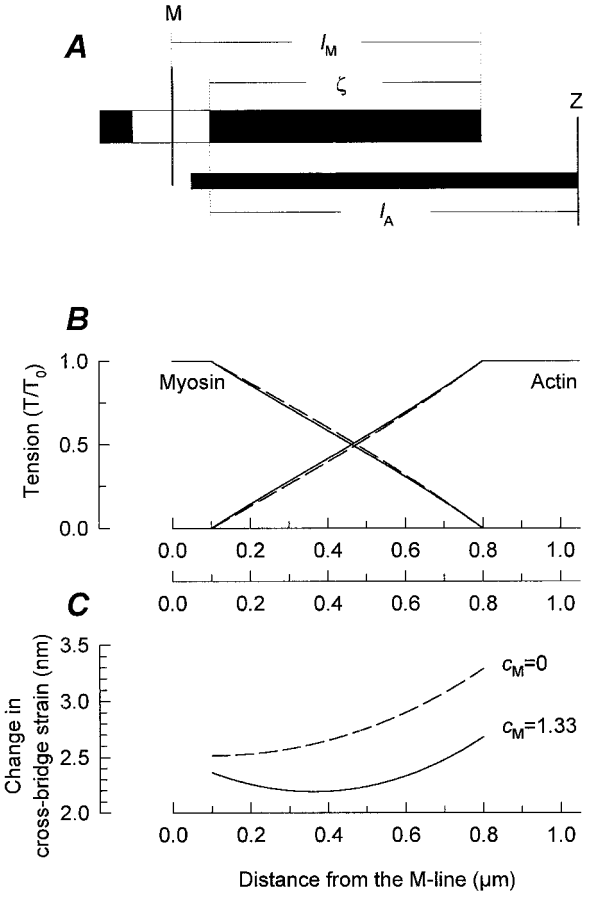

FIGURE 8 Distributed strain in the half-sarcomere. (*A*) Schematic representation of the structure of the half-sarcomere at sarcomere length 2.1 μm. l_M, the length of the myosin filament, is taken as 0.8 μm; ζ, the effective length of the overlap zone, as 0.7 μm; l_A, the length of the actin filament from the Z-line to the beginning of the bare zone, as 0.95 μm. (*B*) Distribution of the change in force along the myosin and the actin filaments when the force is instantaneously increased from zero to T_0. *Dashed line*: c_M = 0 nm $\mu m^{-1}\ T_0^{-1}$; *continuous line*: c_M = 1.33 nm $\mu m^{-1}\ T_0^{-1}$. (*C*) Distribution of the change in cross-bridge strain along the overlap zone for an instantaneous force increase of T_0 with either c_M = 0 (*dashed line*) or c_M = 1.33 nm $\mu m^{-1}\ T_0^{-1}$ (*continuous line*).

the force (T_0) developed at the plateau of the isometric tetanus is given by

$$\bar{S}_A(T_0) = c_A(l_A - \zeta)T_0 + c_A\zeta T_0/2 \qquad (2)$$

The first term arises from the region of the nonoverlapped actin filament and the second from the region where cross-bridges can attach. l_A is the length of the actin filament between the Z-line and the beginning of the bare zone, and ζ is the effective length of the overlap zone (see Appendix and Fig. 8 *A*). At 2.1-μm sarcomere length, l_A = 0.95 μm and ζ = 0.7 μm, and c_A was measured as 2.32 nm $\mu m^{-1}\ T_0^{-1}$, giving $\bar{S}_A(T_0)$ = 1.4 $\pm$ 0.2 nm or 0.15 $\pm$ 0.02% l_A.

This value is significantly smaller than that (0.26%) estimated by x-ray diffraction measurements of changes in the spacing of actin-based reflections from whole muscles of *Rana catesbeiana* (Huxley et al., 1994, temperature 10–14°C;

Wakabayashi et al., 1994, temperature 8–10°C) and from single muscle fibers of *Rana temporaria* (Piazzesi et al., 1997b, temperature 4°C). The larger strain observed in the x-ray experiments may be due to a larger isometric tetanic force per cross-sectional area (T_0) for the temperature and species used in those measurements. In the x-ray experiments on whole muscle, T_0 was probably larger by a factor of 1.2 because of the higher temperature (Woledge et al., 1985). In single fiber experiments at 4°C, T_0 is 1.5 times larger in *Rana temporaria* than in *Rana esculenta* (our unpublished measurements). If we assume that the packing density of filaments within the myofibrils and that of myofibrils within the fiber are the same in different species, these differences in T_0 would lead to different filament strains being measured in the various experiments, even if filament compliance were constant. When the different force per filament in *Rana esculenta* and *Rana temporaria* is taken into account, according to these assumptions, the value of $\bar{S}_A(T_0)$ for *Rana temporaria* predicted from our stiffness measurements is 0.22 ± 0.03% l_A, which is similar to that estimated in the x-ray experiments.

The contribution of actin filament compliance to the half-sarcomere compliance is given by $C_A = c_A(l_A - \frac{2}{3}\zeta)$ (equation A10, Ford et al., 1981; Eq. A1 in the Appendix). C_A at 2.1-μm sarcomere length, $C_{A,0}$, is 1.12 ± 0.17 nm T_0^{-1}. This represents 29 ± 4% of the total half-sarcomere compliance in isometric contraction (3.88 ± 0.07 nm T_0^{-1}) and 44 ± 7% of the total half-sarcomere compliance in rigor (2.56 ± 0.08 nm T_0^{-1}).

The value of 29% for the contribution of actin filaments to half-sarcomere compliance in an isometric tetanus is similar to that measured by Julian and Morgan (1981) in single fibers from *Rana temporaria*, 30%. On the other hand, in other experiments on single fibers from either *Rana temporaria* (Ford et al., 1981) or *Rana esculenta* (Bagni et al., 1990), the fraction of the half-sarcomere compliance attributed to actin filaments in an isometric tetanus was estimated to be less than 20%. The estimate of Ford et al. (1981) was based on the relation between half-sarcomere compliance and sarcomere length in the range of sarcomere lengths between 2.1 and 3.2 μm, where other factors, such as myosin filament compliance and development of sarcomere inhomogeneity, may affect the estimate. The estimate of Bagni et al. (1990) was based on compliance measurements in the sarcomere length range 1.96–2.16 μm, similar to the present work. However, sarcomere length changes were not measured in those experiments, and the tendon compliance assumed (23% of the half-sarcomere compliance) led to an overestimate of the half-sarcomere compliance. Consequently, the contribution of actin filaments to the half-sarcomere compliance was underestimated. Actually, the value of c_A that can be calculated from the slope of the relation between fiber compliance and sarcomere length obtained by Bagni et al. (1990) is ~2 nm μm^{-1} T_0^{-1}, similar to the value reported here (2.32 ± 0.34 nm μm^{-1} T_0^{-1}), as expected according to the conclusion from our work that the slope of the relation is the same, independent of the contribution of tendon compliance.

The value of 44% for the contribution of actin filaments to half-sarcomere compliance in rigor is somewhat lower than that estimated in skinned fibers from rabbit psoas muscle (55%, Higuchi et al., 1995).

Our estimate of actin filament compliance per unit length can be related to the compliance of an individual actin filament by considering the number of filaments per unit cross-sectional area of the fiber. In intact fibers from frog skeletal muscle, taking the d_{10} lattice spacing as 37.5 nm (Matsubara and Elliott, 1972) and the fraction of cross section occupied by myofibrils as 0.83 (Mobley and Eisenberg, 1975), there are 1.02×10^{15} actin filaments m^{-2} of the fiber cross section. With $T_0 = 228 \pm 21$ kN m^{-2} (mean ± SEM, 10 fibers) the compliance per actin filament is 2.32 nm μm^{-1}/(228 kN m^{-2}/1.02×10^{15} filaments m^{-2}) = 10.4 pm pN^{-1} μm^{-1}. This value is slightly lower than both the value measured at similar force levels in rabbit muscle fibers in rigor (14.8 pm pN^{-1} μm^{-1}; Higuchi et al., 1995) and that measured for isolated actin-tropomyosin filaments (15.4 pm pN^{-1} μm^{-1}; Kojima et al., 1994). A larger compliance of the actin filament in skinned rabbit fibers is in agreement with the larger contribution of the actin filament compliance to the half-sarcomere compliance in the measurements of Higuchi et al. (1995) (see above). On the other hand, the lattice spacing and the fractional volume of extramyofibrillar space, and therefore the force per filament, may be different in rabbit and frog muscles.

Compliance of the myosin filaments

The change in spacing of the myosin-based meridional x-ray reflections produced by applying rapid length changes to whole muscles (Huxley et al., 1994) or isolated muscle fibers (Piazzesi et al., 1997b) during an isometric tetanus shows that the myosin filament is extended by ~0.10% for a tension increase of T_0. Larger spacing changes have been observed when tension was altered by applying ramp shortening or lengthening to active muscles (Huxley et al., 1994; Wakabayashi et al., 1994). However, the spacing changes recorded during these slow length changes are likely to contain components that are not related to filament compliance, because cross-bridges can detach from and reattach to actin during the period of the measurements. Other structural changes may contribute to the change in spacing of the myosin-based x-ray reflections under these conditions, as is known to occur during the development of an isometric tetanus (Haselgrove, 1975; Bordas et al., 1993).

Because these myosin-based x-ray reflections arise from the axial periodicity of the myosin heads, the 0.10% spacing change presumably measures the average strain along the whole of the myosin filament, except the bare zone. Taking into account the nearly linear variation of force along the filament (Fig. 8 *B*), the myosin filament compliance per unit length (c_M) can be calculated from the average strain ($\bar{S}_M$)

according to the equation

$$c_M = \bar{S}_M/(\zeta(T_0/2)) \quad (3)$$

$\bar{S}_M$ is calculated as 0.10% multiplied by 700 nm (the length of the overlap zone in the half-sarcomere) T_0^{-1}. Thus $\bar{S}_M$ = 0.7 nm T_0^{-1}, giving c_M = 2 nm μm^{-1} T_0^{-1}. Because T_0 in *Rana temporaria* fibers at 4°C is 1.5 times that in *Rana esculenta* fibers at the same temperature, the best estimate of c_M in the present experiments is 1.33 nm μm^{-1} T_0^{-1}. Using Eq. A1 of the Appendix, the contribution of myosin filament compliance to the half-sarcomere compliance can be calculated as $C_M = c_M(l_M - \frac{2}{3}\zeta)$. C_M at 2.1 μm, $C_{M,0}$, is 0.44 nm, or 11% of the total half-sarcomere compliance.

These estimates of myosin filament compliance are based on the spacings of x-ray reflections that are related to the axial mass distribution of the myosin heads. It is possible that the measured changes in head spacing give an overestimate of the compliance of the myosin filament backbone, because the axial spacing of the heads may be influenced by compliance in the heads themselves, or in the actin filament.

Compliance of the cross-bridges

To discriminate the contributions of the cross-bridges from those of the other structural components to the total half-sarcomere compliance, C_0 in Eq. 1 must be made explicit. According to Eq. A4 in the Appendix, and assuming that the compliance of the Z-line, C_Z, is zero, C_0 is given by

$$C_0 = \left\{c_A\left(\frac{1}{3}\zeta - l_M + \frac{s_0}{2}\right) + c_M\left(l_M - \frac{2}{3}\zeta\right) + \frac{1}{\beta k_0 \zeta}\right\} \quad (4)$$

where l_M is the length of the myosin filament, β is the fraction of myosin cross-bridges attached to the actin filament, and k_0 is the stiffness of cross-bridges per unit length when all cross-bridges are attached.

Because of the uncertainties of the current estimate of myosin filament compliance (see previous section), the following analysis is made, assuming two limiting conditions for the value of c_M: 0 and 1.33 nm μm^{-1} T_0^{-1}. If the myosin filament compliance is zero ($c_M = 0$), Eq. 4 reduces to

$$C_0 = c_A\left(\frac{1}{3}\zeta - l_M + \frac{s_0}{2}\right) + \frac{1}{\beta k_0 \zeta} \quad (5)$$

In rigor, we further assume that all myosin heads are attached to actin (Cooke and Franks, 1980; Thomas and Cooke, 1980; Lovell et al., 1981), so $\beta = 1$. Thus the only unknown parameter in Eq. 5 is k_0. Substituting $C_0 = 2.56 \pm 0.08$ nm T_0^{-1} (Fig. 7), $c_A = 2.32 \pm 0.34$ nm μm^{-1} T_0^{-1}, $\zeta = 0.7$ μm, and $l_M = 0.8$ μm gives $k_0 = 0.99 \pm 0.13$ T_0 nm^{-1} μm^{-1}, and the cross-bridge compliance ($1/k_0\zeta$) is ($1/(0.99\ T_0\ nm^{-1}\ \mu m^{-1} \times 0.7\ \mu m)$ =) 1.44 ± 0.18 nm T_0^{-1}.

The value of β in active contraction can be calculated from the values of C_0 in active contraction (3.88 ± 0.05 nm T_0^{-1}) and rigor (2.56 ± 0.08 nm T_0^{-1}), using Eq. A6 in the Appendix, under the assumption that the compliances of the myosin filament and Z-line are zero. This gives $\beta = 0.52 \pm 0.04$, i.e., 52% of the cross-bridges attached in rigor would be attached in isometric contraction. If $c_M = 1.33$ nm μm^{-1} T_0^{-1}, the upper limit according to the previous section, Eq. 4 gives $k_0 = 1.44 \pm 0.33$ T_0 nm^{-1} μm^{-1}, and consequently in rigor the compliance of the cross-bridges ($1/k_0\zeta$) is 1.01 ± 0.23 nm T_0^{-1}. In this case, from Eq. A6 in the Appendix, at the plateau of the isometric tetanus, $\beta = 0.43 \pm 0.05$ and the cross-bridge compliance ($1/\beta k_0\zeta$) is 2.30 ± 0.43 nm T_0^{-1} (note that the value of β decreases with increasing c_M). These values would have been slightly underestimated if the value of c_M from the x-ray diffraction measurements had been an overestimate, as discussed in the previous section.

In an active muscle fiber at the tetanus plateau, ~40% of the total compliance per half-sarcomere is in the myofilaments. Consequently, the change in strain of the cross-bridges for an instantaneous change of tension from zero to T_0 varies according to their position along the overlap zone. The distribution of the change of cross-bridge strain, determined by the procedure described in Appendix A of Ford et al. (1981), is shown in Fig. 8 *C* for both $c_M = 0$ (*dashed line*) and $c_M = 1.33$ nm μm^{-1} T_0^{-1} (*continuous line*). In the former case the cross-bridge strain increases with distance from the M-line, over the range 2.51–3.29 nm. Cross-bridges nearer the M-line have a smaller strain because more of the applied strain is taken up by the longer segment of actin filament that is mechanically in series with them.

If the myosin filament is also compliant, both the average value and the range of the cross-bridge strain are reduced, and the minimum strain occurs within the overlap region. With $c_M = 1.33$ nm μm^{-1} T_0^{-1} (*continuous line* in Fig. 8 *C*), the cross-bridge strain is in the range 2.19–2.68 nm, and the minimum value occurs at 0.36 μm from the M-line.

These calculations take no account of the active response of the cross-bridges, i.e., force generation within the cross-bridge, or attachment to or detachment from actin in response to a length change. Fig. 8 *C* represents the distribution of the change in elastic strain that would be produced by a change in tension of T_0, but this is unlikely to correspond to the actual distribution of strain at the plateau of an isometric tetanus. At the tetanus plateau the steady tension is maintained by asynchronous cross-bridge interactions. Freshly attached cross-bridges must generate force against their own compliance, without significant change in actin filament strain. In this situation the strain in the attached cross-bridges would be independent of the distance from the M-line, and would take the value ($1/(\beta k_0\zeta) \times T_0$ =) 2.30 ± 0.43 nm for $c_M = 1.33$ nm μm^{-1} T_0^{-1}.

This value is not significantly different from the maximum extent of reversal of the working stroke (2 nm; Piazzesi et al., 1997c), which corresponds to the size of the structural change in the cross-bridge that was responsible for the generation of isometric force. This conclusion strongly supports the idea, assumed in the original theory of

Huxley and Simmons (1971), that the structural change leading to isometric force generation is completely reversible.

Fraction of cross-bridges attached at the isometric tetanus plateau

The present results imply that the fraction of myosin cross-bridges attached to actin in isometric contraction, assuming that all are attached and bearing tension in rigor and that c_M is 1.33 nm μm^{-1} T_0^{-1}, is 0.43 ± 0.05. If not all cross-bridges were attached and bearing tension in rigor, the above estimate would represent the relative fraction in the isometric contraction compared to rigor.

The fraction of myosin heads attached to actin during active contraction has previously been estimated from a variety of structural methods by comparing values of structural parameters in relaxation, active contraction, and rigor. The intensities of the equatorial x-ray reflections in contracting muscle are much closer to the rigor than to the relaxed values, suggesting that up to 90% of the myosin heads are close to the actin filaments (Haselgrove and Huxley, 1973; Huxley and Kress, 1985). However, the large changes in these x-ray reflections on activation may be due to movements of the myosin heads associated with the regulation of contraction, or with a weak interaction between the heads and actin that does not contribute to stiffness or active force (Huxley and Kress, 1985). The low-angle x-ray reflections arising from the actin helix are much weaker in active contraction than in rigor (Huxley et al., 1982), suggesting that in active contraction only a small fraction of the heads, probably less than 30%, take up the rigor conformation. The orientation of spin probes on the catalytic domain of myosin heads in skinned muscle fibers in relaxation, active contraction, and rigor (Cooke et al., 1982; Ostap et al., 1995) suggest that in active contraction 20–30% of the myosin heads are in the rigor conformation. These estimates are somewhat lower than the 43% of cross-bridges attached to actin in isometric contraction, compared to rigor, estimated from the present stiffness data. A difference in this direction would be expected if the rigor orientation corresponds to that taken up by cross-bridges at the end of the working stroke, whereas the majority of heads attached in an isometric contraction are in a structurally distinct state at the beginning of the working stroke (Huxley and Tideswell, 1997; Linari et al., 1997; Lombardi et al., 1995; Piazzesi et al., 1995). In fact, this distinction may produce a much larger difference between the fraction of attached cross-bridges and the fraction of a rigor-like conformation than that noted above, depending on the structure of the state at the beginning of the working stroke.

The average force exerted by each attached myosin head at the plateau of the isometric tetanus can be calculated as $T_0/(NHf)$, where T_0 is 228 kN m^{-2} in the present experiments; N, the density of myosin filaments, is 0.51×10^{15} m^{-2}, one-half of the value estimated above for the actin filaments; H, the number of myosin heads per half-filament, is 290; and f is the fraction of myosin heads attached to actin in isometric contraction. With $f = 0.43$, the average force per attached head is 3.6 pN, which is similar to the average values of force developed by single myosin heads at high load in in vitro motility assays (Finer et al., 1994; Ishijima et al., 1994; Molloy et al., 1995), although substantially lower than the peak values reported in the first two of these studies.

Using this value of the average force per myosin head, the mechanical energy produced in the working stroke can be estimated from the T_2 curve (Huxley and Simmons, 1971; Piazzesi and Lombardi, 1995), taking into account the reduction of the intercept of this curve on the length axis to ~10 nm due to filament compliance. This gives the energy per working stroke as 27×10^{-21} J, which is ~44% of the free energy available from ATP hydrolysis ($\sim 60 \times 10^{-21}$ J, assuming that the efficiency of energy transduction is 60%). This value is consistent with the possibility that more than one working stroke could be produced per ATP hydrolyzed (Ishijima et al., 1991; Lombardi et al., 1992).

APPENDIX

The contributions of the actin and myosin filaments and the myosin cross-bridges to the total half-sarcomere compliance were calculated by using equation A10 of Ford et al. (1981):

$$C = c_A\left(l_A - \frac{2}{3}\zeta\right) + c_M\left(l_M - \frac{2}{3}\zeta\right) + \frac{1}{k_c\zeta} + C_Z \qquad \text{(A1)}$$

where c_A is the compliance of the actin filament per unit length; l_A is the effective actin filament length, i.e., the length of the actin filament from the Z-line to the beginning of the bare zone (see Fig. 8 *A*); ζ is the effective length of the overlap zone between myosin and actin filaments (not including the bare zone); c_M is the compliance of myosin filament per unit length; l_M is the length of the myosin filament including the bare zone; k_c is the stiffness of the cross-bridges per unit length; and C_Z is the compliance of the Z-line. This equation is a good approximation of the exact solution for the parameter values used here. In the sarcomere length range 2.00–2.15 μm, ζ takes the constant value of 0.7 μm, l_M and k_c are constant, and the only parameter on the right-hand side of Eq. A1 that depends on sarcomere length (s) is l_A. According to Fig. 8 *A*, this can be expressed as

$$l_A = \frac{s}{2} - l_M + \zeta \qquad \text{(A2)}$$

To take into account a variable fraction of myosin cross-bridges attached to actin, k_c can be expressed as the product of k_0, the cross-bridge stiffness per unit length when all of the cross-bridges are attached and exhibit full stiffness, and β, which varies between 0 (no cross-bridges attached) and 1 (all of the cross-bridges attached). Thus the half-sarcomere compliance, C, can be written as

$$C = \frac{c_A}{2}s + \left\{c_A\left(\frac{1}{3}\zeta - l_M\right) + c_M\left(l_M - \frac{2}{3}\zeta\right) + \frac{1}{\beta k_0\zeta} + C_Z\right\} \qquad \text{(A3)}$$

A plot of C against s should therefore be a straight line with slope $c_A/2$. The intercept on the y axis, corresponding to the term in the curly brackets, is the sum of the contributions to C of the structural components that do not depend on sarcomere length in the range considered here. If s_0 is the reference

sarcomere length of 2.1 μm, it is convenient to rewrite Eq. A3 as

$$C = \frac{c_A}{2}(s - s_0) + \left\{ c_A\left(\frac{1}{3}\zeta - l_M + \frac{s_0}{2}\right) + c_M\left(l_M - \frac{2}{3}\zeta\right) + \frac{1}{\beta k_0 \zeta} + C_Z \right\} \tag{A4}$$

so that the term in brackets is the value of C at s_0, termed C_0.

We assume that under the conditions of our experiments in rigor, all of the cross-bridges are attached and exhibit full stiffness, so that $k_c = k_0$. Writing $C_{0,r}$ and $C_{0,t}$ for the values of C_0 for rigor and the isometric tetanus, respectively,

$$k_0 = \left\{ \left[C_{0,r} - c_A\left(\frac{1}{3}\zeta - l_M + \frac{s_0}{2}\right) - c_M\left(l_M - \frac{2}{3}\zeta\right) - C_Z \right]\zeta \right\}^{-1} \tag{A5a}$$

for rigor, and

$$\beta k_0 = \left\{ \left[C_{0,t} - c_A\left(\frac{1}{3}\zeta - l_M + \frac{s_0}{2}\right) - c_M\left(l_M - \frac{2}{3}\zeta\right) - C_Z \right]\zeta \right\}^{-1} \tag{A5b}$$

for the isometric tetanus. Thus β can be derived as

$$\beta = \frac{C_{0,r} - c_A\left(\frac{1}{3}\zeta - l_M + \frac{s_0}{2}\right) - c_M\left(l_M - \frac{2}{3}\zeta\right) - C_Z}{C_{0,t} - c_A\left(\frac{1}{3}\zeta - l_M + \frac{s_0}{2}\right) - c_M\left(l_M - \frac{2}{3}\zeta\right) - C_Z} \tag{A6}$$

The authors thank Prof. Sir Andrew Huxley for helpful criticisms on the manuscript, Mr. A. Aiazzi and Mr. M. Dolfi for skilled technical assistance, and Mr. A. Vannucchi for preparing the illustrations.

This work was supported by grants from Telethon (no. 945), the Consiglio Nazionale delle Ricerche (Italy), the Ministero dell'Università e della Ricerca Scientifica e Tecnologica (Italy), the Medical Research Council (UK), and the European Community.

REFERENCES

Bagni, M. A., G. Cecchi, F. Colomo, and C. Poggesi. 1990. Tension and stiffness of frog muscle fibres at full filament overlap. *J. Muscle Res. Cell Motil.* 11:371–377.

Bagni, M. A., G. Cecchi, F. Colomo, and C. Tesi. 1988. Plateau and descending limb of the sarcomere length-tension relation in short length-clamped segments of frog muscle fibres. *J. Physiol. (Lond.).* 401: 581–595.

Bagni, M. A., G. Cecchi, P. J. Griffiths, Y. Maeda, G. Rapp, and C. C. Ashley. 1994. Lattice spacing changes accompanying isometric tension development in intact single muscle fibres. *Biophys. J.* 67:1965–1975.

Bershitsky, S. Y., and A. K. Tsaturyan. 1995. Force generation and work production by covalently cross-linked actin-myosin cross-bridges in rabbit muscle fibers. *Biophys. J.* 69:1011–1021.

Bordas, J., G. P. Diakun, F. G. Diaz, J. E. Harries, R. A. Lewis, J. Lowy, G. R. Mant, M. L. Martin-Fernandez, and E. Towns-Andrews. 1993. Two-dimensional time-resolved X-ray diffraction studies of live isometrically contracting frog sartorius muscle. *J. Muscle Res. Cell Motil.* 14:311–324.

Cecchi, G., F. Colomo, and V. Lombardi. 1976. A loudspeaker servo-system for determination of mechanical characteristics of isolated muscle fibres. *Boll. Soc. Ital. Biol. Sper.* 52:733–736.

Cooke, R., M. S. Crowder, and D. D. Thomas. 1982. Orientation of spin labels attached to cross-bridges in contracting muscle fibers. *Nature.* 300:776–778.

Cooke, R., and K. Franks. 1980. All myosin heads form bonds with actin in rigor rabbit skeletal muscle. *Biochemistry.* 19:2265–2269.

Finer, J. T., R. M. Simmons, and J. A. Spudich. 1994. Single myosin molecule mechanics: piconewton forces and nanometre steps. *Nature.* 368:113–119.

Ford, L. E., A. F. Huxley, and R. M. Simmons. 1977. Tension responses to sudden length change in stimulated frog muscle fibres near slack length. *J. Physiol. (Lond.).* 269:441–515.

Ford, L. E., A. F. Huxley, and R. M. Simmons. 1981. The relation between stiffness and filament overlap in stimulated frog muscle fibres. *J. Physiol. (Lond.).* 311:219–249.

Goldman, Y. E., and A. F. Huxley. 1994. Actin compliance: are you pulling my chain? *Biophys. J.* 67:2131–2136.

Goldman, Y. E., and R. M. Simmons. 1977. Active and rigor muscle stiffness. *J. Physiol. (Lond.).* 269:55P–57P.

Goldman, Y. E., and R. M. Simmons. 1986. The stiffness of frog skinned muscle fibres at altered lateral filament spacing. *J. Physiol. (Lond.).* 378:175–194.

Gordon, A. M., A. F. Huxley, and F. J. Julian. 1966. The variation in isometric tension with sarcomere length in vertebrate muscle fibres. *J. Physiol. (Lond.).* 184:170–192.

Haselgrove, J. C. 1975. X-ray evidence for conformational changes in the myosin filaments of vertebrate striated muscle. *J. Mol. Biol.* 92:113–143.

Haselgrove, J. C., and H. E. Huxley. 1973. X-ray evidence for radial cross-bridge movement and for the sliding filament model in actively contracting muscle. *J. Mol. Biol.* 77:549–568.

Higuchi, H., T. Yanagida, and Y. E. Goldman. 1995. Compliance of thin filaments in skinned fibers of rabbit skeletal muscle. *Biophys. J.* 69: 1000–1010.

Huxley, A. F. 1980. Reflections on Muscle. The Sherrington Lectures XIV, Liverpool University Press, Liverpool.

Huxley, A. F., and V. Lombardi. 1980. A sensitive force transducer with resonant frequency 50 kHz. *J. Physiol. (Lond.).* 305:15P–16P.

Huxley, A. F., V. Lombardi, and L. D. Peachey. 1981. A system for fast recording of longitudinal displacement of a striated muscle fibre. *J. Physiol. (Lond.).* 317:12P–13P.

Huxley, A. F., and R. M. Simmons. 1971. Proposed mechanism of force generation in striated muscle. *Nature.* 233:533–538.

Huxley, A. F., and S. Tideswell. 1996. Filament compliance and tension transients in muscle. *J. Muscle Res. Cell Motil.* 17:507–511.

Huxley, A. F., and S. Tideswell. 1997. Rapid regeneration of power stroke in contracting muscle by attachment of second myosin head. *J. Muscle Res. Cell Motil.* 18:111–114.

Huxley, H. E., A. R. Faruqi, M. Kress, J. Bordas, and M. H. J. Koch. 1982. Time resolved x-ray diffraction studies of the myosin layer line reflections during muscle contraction. *J. Mol. Biol.* 158:673–684.

Huxley, H. E., and M. Kress. 1985. Crossbridge behaviour during muscle contraction. *J. Muscle Res. Cell Motil.* 6:153–161.

Huxley, H. E., A. Stewart, H. Sosa, and T. Irving. 1994. X-ray diffraction measurements of the extensibility of actin and myosin filaments in contracting muscle. *Biophys. J.* 67:2411–2421.

Irving, M. 1995. Give in the filaments. *Nature.* 374:14–15.

Ishijima, A., T. Doi, K. Sakurada, and T. Yanagida. 1991. Sub-piconewton force fluctuations of actomyosin in vitro. *Nature.* 352:301–306.

Ishijima, A., Y. Harada, H. Kojima, T. Funatzu, H. Higuchi, and T. Yanagida. 1994. Single-molecule analysis of the actomyosin motor using nano-manipulation. *Biochem. Biophys. Res. Commun.* 199: 1057–1063.

Julian, F. J., and D. L. Morgan. 1981. Tension, stiffness, unloaded shortening speed and potentiation of frog muscle fibres at sarcomere lengths below optimum. *J. Physiol. (Lond.).* 319:205–217.

Kojima, H., A. Ishijima, and T. Yanagida. 1994. Direct measurement of stiffness of single actin filaments with and without tropomyosin using in vitro nano-manipulation. *Proc. Natl. Acad. Sci. USA.* 91:12962–12966.

Linari, M., A. Aiazzi, M. Dolfi, G. Piazzesi, and V. Lombardi. 1993. A system for studying tension transients in segments of skinned muscle fibres from rabbit psoas. *J. Physiol. (Lond.).* 473:8P.

Linari, M., V. Lombardi, and G. Piazzesi. 1997. Cross-bridge kinetics studied with staircase shortening in single fibres from skeletal muscle. *J. Muscle Res. Cell Motil.* 18:91–101.

Linari, M., and R. C. Woledge. 1995. Comparison of energy output during ramp and staircase shortening in frog muscle fibres. *J. Physiol. (Lond.).* 487:699–710.

Lombardi, V., and G. Piazzesi. 1990. The contractile response during steady lengthening of stimulated frog muscle fibres. *J. Physiol. (Lond.).* 431:141–171.

Lombardi, V., G. Piazzesi, M. A. Ferenczi, H. Thirlwell, I. Dobbie, and M. Irving. 1995. Elastic distortion of myosin heads and repriming of the working stroke in muscle. *Nature.* 374:553–555.

Lombardi, V., G. Piazzesi, and M. Linari. 1992. Rapid regeneration of the actin-myosin power stroke in contracting muscle. *Nature.* 355:638–641.

Lovell, S. J., P. J. Knight, and W. F. Harrington. 1981. Fraction of myosin heads bound to thin filaments in rigor fibrils from insect flight and vertebrate muscles. *Nature.* 293:664–666.

Månsson, A. 1993. Tension transients in skeletal muscle fibres at varied tonicity of the extracellular medium. *Biophys. J.* 14:15–25.

Matsubara, I., and G. F. Elliott. 1972. X-ray diffraction studies on skinned single fibres of frog skeletal muscle. *J. Mol. Biol.* 72:657–669.

Mobley, B. A., and B. R. Eisenberg. 1975. Sizes of components in frog skeletal muscle measured by methods of stereology. *J. Gen. Physiol.* 66:31–45.

Molloy, J. E., J. E. Burns, J. Kendrick-Jones, R. T. Tregear, and D. C. S. White. 1995. Movement and force produced by a single myosin head. *Nature.* 378:209–212.

Nishiye, E., A. V. Somlyo, K. Török, and A. P. Somlyo. 1993. The effect of MgADP on cross-bridge kinetics: a laser flash photolysis study of guinea pig smooth muscle. *J. Physiol. (Lond.).* 460:247–271.

Ostap, E. M., V. A. Barnett, and D. D. Thomas. 1995. Resolution of three structural states of spin-labeled myosin in contracting muscle. *Biophys. J.* 69:177–188.

Piazzesi, G., F. Francini, M. Linari, and V. Lombardi. 1992. Tension transients during steady lengthening of tetanized muscle fibres of the frog. *J. Physiol. (Lond.).* 445:659–711.

Piazzesi, G., N. Koubassova, I. Dobbie, M. Linari, M. Reconditi, M. A. Ferenczi, M. Irving, and V. Lombardi. 1997a. Location of the cross-bridge compliance: mechanical and x-ray diffraction measurements in single muscle fibres. XXVI European Muscle Conference, 21–26 September 1997. *J. Muscle Res. Cell Motil.* (in press).

Piazzesi, G., N. Koubassova, M. Reconditi, I. Dobbie, M. A. Ferenczi, V. Lombardi, and M. Irving. 1997b. Cross-bridge and filament compliance measured by x-ray diffraction in single frog muscle fibres. *Pflügers Arch.* 434:R57–34.

Piazzesi, G., M. Linari, and V. Lombardi. 1994. The effect of hypertonicity on force generation in tetanized single fibres from frog skeletal muscle. *J. Physiol. (Lond.).* 476:531–546.

Piazzesi, G., M. Linari, M. Reconditi, F. Vanzi, and V. Lombardi. 1997c. Cross-bridge detachment and attachment following a step stretch imposed on active single frog muscle fibres. *J. Physiol. (Lond.).* 498:3–15.

Piazzesi, G., and V. Lombardi. 1995. A cross-bridge model that is able to explain mechanical and energetic properties of shortening muscle. *Biophys. J.* 68:1966–1979.

Piazzesi, G., V. Lombardi, M. A. Ferenczi, H. Thirlwell, I. Dobbie, and M. Irving. 1995. Changes in the x-ray diffraction pattern from single, intact muscle fibers produced by rapid shortening and stretch. *Biophys. J.* 68:92s–98s.

Reedy, M. K., K. C. Holmes, and R. T. Tregear. 1965. Induced changes in orientation of the cross-bridges of glycerinated insect flight muscle. *Nature.* 207:1276–1280.

Thomas, D. D., and R. Cooke. 1980. Orientation of spin-labeled myosin heads in glycerinated muscle fibers. *Biophys. J.* 32:891–906.

Wakabayashi, K., Y. Sugimoto, H. Tanaka, Y. Ueno, Y. Takezawa, and Y. Amemiya. 1994. X-ray diffraction evidence for the extensibility of actin and myosin filaments during muscle contraction. *Biophys. J.* 67: 2422–2435.

Woledge, R. C., N. A. Curtin, and E. Homsher. 1985. Energetic Aspects of Muscle Contraction. Academic Press, London.

Yamamoto, T., and J. W. Herzig. 1978. Series elastic properties of skinned muscle fibres in contraction and rigor. *Pflügers Arch.* 373:21–24.